A EUROPEAN JOURNAL

CHEMPHYSCHEM

OF CHEMICAL PHYSICS AND PHYSICAL CHEMISTRY

Accepted Article

Title: Continuous Radio Amplification by Stimulated Emission of Radiation using Parahydrogen Induced Polarization (PHIP-RASER) at 14 Tesla

Authors: Andrey Pravdivtsev, Frank D. Sönnichsen, and Jan-Bernd Hövener

To be cited as: *ChemPhysChem* 10.1002/cphc.201901056

Link to VoR: http://dx.doi.org/10.1002/cphc.201901056

A Journal of ChemPubSoc Europe

WILEY-VCH www.chemphyschem.org

Continuous Radio Amplification by Stimulated Emission of Radiation using Parahydrogen Induced Polarization (PHIP-RASER) at 14 Tesla

Andrey N. Pravdivtsev,*[a] Frank D. Sönnichsen[b] and Jan-Bernd Hövener*[a]

Abstract: Nuclear Magnetic Resonance (NMR) is an intriguing quantum-mechanical effect that is used for daily life medical diagnostics and chemical analysis alike. Numerous advancements have contributed to the success of the technique, including hyperpolarized contrast agents that enable real-time imaging of metabolism in vivo. Here, we report the finding of an NMR radio amplification by stimulated emission of radiation (RASER), which continuously emits ^{1}H NMR signal for more than 10 min. Based on parahydrogen induced hyperpolarization (PHIP, 50 % para-enrichment), PHIP-RASER is expected to be functional in a wide range of frequencies (10^1 – 10^3 MHz) and was demonstrated at 600 MHz. PHIP-RASER occurred spontaneously upon supply of $p\mathrm{H}_2$ to a solution containing a hydrogenation catalyst and unsaturated molecule, or was triggered with a standard NMR excitation pulse. Full chemical shift resolution was maintained and a linewidth of 0.6 ppb was achieved, despite apparent inhomogeneities from supplying $p\mathrm{H}_2$. The effect was reproduced by simulating a weakly coupled, two spin-½ system with superoperators. All equipment used was standard issue, such that the effect can be reproduced by any NMR lab worldwide with access to liquid nitrogen for producing parahydrogen.

Introduction

The quest for a continuously emitting, high-frequency, liquid-state radio amplification by stimulated emission (RASER) at MHz frequencies and above is ongoing for more than a decade. Pioneering work demonstrated RASERs at low fields with resonance frequencies from 10 Hz to 50 kHz, based on ^{3}He or ^{129}Xe gases polarized with Spin Exchange Optical Pumping (SEOP),[1,2] for hours[3,4] or days. These techniques were used, among others, for probing fundamental symmetries.[5]

A 400 MHz RASER was accomplished by Dissolution Dynamic Nuclear Polarization (dDNP)[6,7], although only for a single shot experiment: RASER signal bursts were observed for three seconds after a hyperpolarized sample was poured into a cavity.[8] Continuous emission of the NMR signal is not feasible with this approach because of relaxation and long sample preparation time.

Closest to a continuous emission at high-frequency was likely a ^{129}Xe RASER, where 11 bursts were observed at 11.7 T (139 MHz) for 8.5 min. Because the polarization was not refreshed, the amplitude was continuously decaying. Interestingly, the magnetization of the sample was so strong that its Larmor frequency was elevated by 3 Hz at the beginning of the experiment due to strong distant dipolar fields.[9]

In a recent breakthrough, Süfke *et al.*[10] demonstrated a continuous NMR RASER based on a combination of innovative hardware[11] and the continuous hyperpolarization[12] provided by Signal Amplification By Reversible exchange[13] (SABRE): SABRE-RASER.[14] Using a sophisticated setup, a spectral resolution of 0.6 Hz was achieved at ≈ 3.8 mT (≈ 4 ppm). This unprecedented resolution of J-couplings was reported, but chemical shift resolution was not possible because of the low magnetic field.[10,14] A transfer of this method to higher fields is not feasible because a level anticrossing (LAC) is required for spontaneous polarization transfer to occur (for ^{1}H, ≈ mT).[15,16] Spontaneous SABRE was reported at higher fields, too, but only with a very small polarizations.[17,18] Continuous high-field Radio Frequency (RF) driven SABRE polarization transfer techniques still provided only moderate and semi-continuous polarization.[19–21]

Results and Discussion

Here, we present a liquid-state NMR RASER that continuously emits RF-signal for any given time at room temperature and 600 MHz (Fig 1 and 2) and under the conditions described below. Using parahydrogen-induced hyperpolarization (PHIP), the RASER begins spontaneously or can be triggered with a standard NMR pulse.

Similar to SABRE-RASER,[10] this new effect is based on the spin order of parahydrogen ($p\mathrm{H}_2$) (eq. 1),

$$\hat{\rho}_{pH_2} = \frac{\hat{1}}{4} - \hat{\mathbf{I}}_1 \cdot \hat{\mathbf{I}}_2, \quad (1)$$

which is continuously supplied to a liquid sample (Fig 1B, 2B).[22]

Elegantly, $p\mathrm{H}_2$ has spin 0, hence does not have magnetization and is impervious to any excitation in its molecular state. Thus, the reservoir of spin order is not affected by pulses or the RASER effect, which takes place in the same physical location.

---

[a] Dr. A. N. Pravdivtsev and Prof. Dr. J.-B. Hövener
Section Biomedical Imaging, Molecular Imaging North Competence Center (MOIN CC), Department of Radiology and Neuroradiology, University Medical Center Kiel, Kiel University,
Am Botanischen Garten 14, 24114, Kiel, Germany
E-mails: andrey.pravdivtsev@rad.uni-kiel.de
jan.hoevener@rad.uni-kiel.de
[b] Prof. Dr. F. Sönnichsen
Otto Diels Institute for Organic Chemistry, Kiel University,
Otto Hahn Platz 5, 24098, Kiel, Germany

Supporting information for this article is given via a link at the end of the document.

10.1002/cphc.201901056

The production of pH_2 is well established, requiring no more than H_2 gas flowing through a porous catalyst at low temperature.[23–25] Stored appropriately, pH_2 is stable for days to weeks.[26] H_2 can be purchased or produced on-site chemically or by electrolysis.[27]

In contrast to SABRE-RASER,[10] here, pH_2 is permanently incorporated into target molecules via homogeneous hydrogenation (Fig 1A and 2A). The catalytic activity was chosen such that only a small fraction of all precursor molecules is hydrogenated at a time. This way, the reaction was upheld for an extended period of time, and PHIP-RASER occurred.

Here, we demonstrated PHIP-RASER for two molecules: ethyl cinnamate and methyl acrylate, for our purposes approximately an AX, 2 spin-½ system and an AMX, 3 spin-½ system.

The 600 MHz emission of the RASER began spontaneously approx. 1.5 min after injection of pH_2, or instantaneously after a single “trigger” excitation pulse of 45° (Fig 1, 2). The “trigger” RF-pulse converted hyperpolarization into transverse magnetization, which, in turn, induced continuous radiation in a few seconds. The “spontaneous” onset of PHIP-RASER required a finite hydrogenation time for the accumulation of a hyperpolarized product.

NMR-RASER data was acquired for a much longer time period than the usual NMR signal. The duration of the emission (here > 10 min) is limited only by pH_2 supply, the hydrogenation catalyst and the reservoir of receiver molecules. In the current implementation, only pH_2 was continuously renewed, but refreshing all constituents can be easily accomplished using a flow setup.[28,29]

After the Fourier transformation of ≈ 10 min RASER signal, two narrow lines were observed at the positions of the added hydrogens, in addition to less pronounced satellites (details of signal processing are given in methods). The line shapes were irregular with a varying full width at half maximum (FWHM) of e.g. ≈ 0.6 ppb (≈ 0.4 Hz, Fig 1D) and ≈ 7.8 ppb (≈ 4.7 Hz, Fig 2D). The reason for the difference in line width may be attributed to varying field homogeneity during pH_2 injection and the different spin systems, but will have to be investigated elsewhere. Note, that no information about the J-coupling network in both 2 and 3 spin-½ systems of ethyl cinnamate and methyl acrylate were revealed in these RASER experiments (Fig 1D, 2D). At the same time, the resonances of the thermally polarized solvent exhibited an inhomogeneously broadened line with FWHM > 20 Hz, (Fig S4). Thus it remains unclear, how much of the sample actually emitted RASER signal. In the absence of these inhomogeneities and magnetic field drift (no lock was applied), the lower limit for the RASER line width is the nominal spectral resolution of the order of 1 mHz for 11 min. A better homogeneity may be achieved in the future by using more sophisticated techniques to dissolve pH_2[30–32] and is currently under investigation. A pH_2 supply that does not disturb the homogeneity of the magnetic field will be instrumental to elucidate PHIP-RASER effect further (compare Fig 1E and Fig S3).

Importantly, we expect that PHIP-RASER is functional at all (high) magnetic field strengths, where parahydrogen and synthesis allows dramatically enhanced nuclear alignment (PASADENA)[33] - although the spectral appearance depends on the radiation damping rate, polarization level and build-up rate (Fig S3, S9, S10).[14] PASADENA conditions are met if the J-coupling between the added hydrogens is weak compared to their chemical shift difference; for J ≈ 10 Hz and chemical shift difference of 1 ppm, this condition is fulfilled at fields > 0.2 T, i.e. at ^1H frequencies above 10 MHz.

Interestingly, the frequency difference between the RASER lines (ζ) was found to differ from their nominal chemical shift difference ($\Delta\delta$). At the same time, several equidistant satellite resonances with the same spacing ζ were found (Fig 1E and 2E).[14] Their location depends on the radiation damping rate relative to the chemical shift difference (Fig S8).[14] Another type of satellites exhibited a more complex structure that strongly depended on experimental settings, not unlike the spectral clustering effect caused by a distant dipolar field.[34] The high level of magnetization also caused a change of the local magnetic field and thus a frequency drift of the resonances (Fig S9).[9,34] All these findings were well reproduced by simulations, as described below. All simulations were performed using the MOIN spin library; the source code is available online.[35,36]

The interaction between the highly polarized system and RF-cavity is essential for the RASER emission.[3–5,10,11] This interaction reveals itself as radiation damping. The radiation damping rate is defined as $(\tau_{RD})^{-1}=\frac{\mu_0}{4}\hbar\gamma^2\eta Q c_s|P|$, where μ_0 is the vacuum permeability, $\hbar$ is the reduced Planck constant, γ is the gyromagnetic ratio, Q is the quality factor of the coil with a filling factor η, c_s is the concentration of the nuclear spin and P is the longitudinal polarization.[37] This definition of radiation damping rate is very convenient for experiments with large magnetizations in thermal equilibrium that can be described simply with modified Bloch equations, or, in a more advanced way, with single- or multi-mode LASER/RASER equations.[14]

All experiments in this paper were conducted with a cryogenically cooled coil with high Q ≈ 500 (see SI). The question arises, if the effect can be reproduced with a conventional coil, too. According to the theory of radiation damping, only the filling factor, the Q-factor of the coil and size of the magnetization are important. Thus, it appears plausible to observe PHIP-RASER with a high resolution NMR coil at room temperature with a Q > 100, but the experimental proof has yet to be established. Note that no RASER was observed when continuous SABRE was reported at ≈ 5 mT, ≈ 10 % filling factor and a Q ≈ $10^{1\text{-}2}$.[12,38]

To elucidate this remarkable effect further, we set out to simulate PHIP-RASER in a coupled two spin-½ system using the density matrix approach and Liouville-von Neumann equation (LvN, eq. S8). It is the most convenient and precise method to simulate liquid state NMR-experiments with coupled multi-spin systems.

10.1002/cphc.201901056

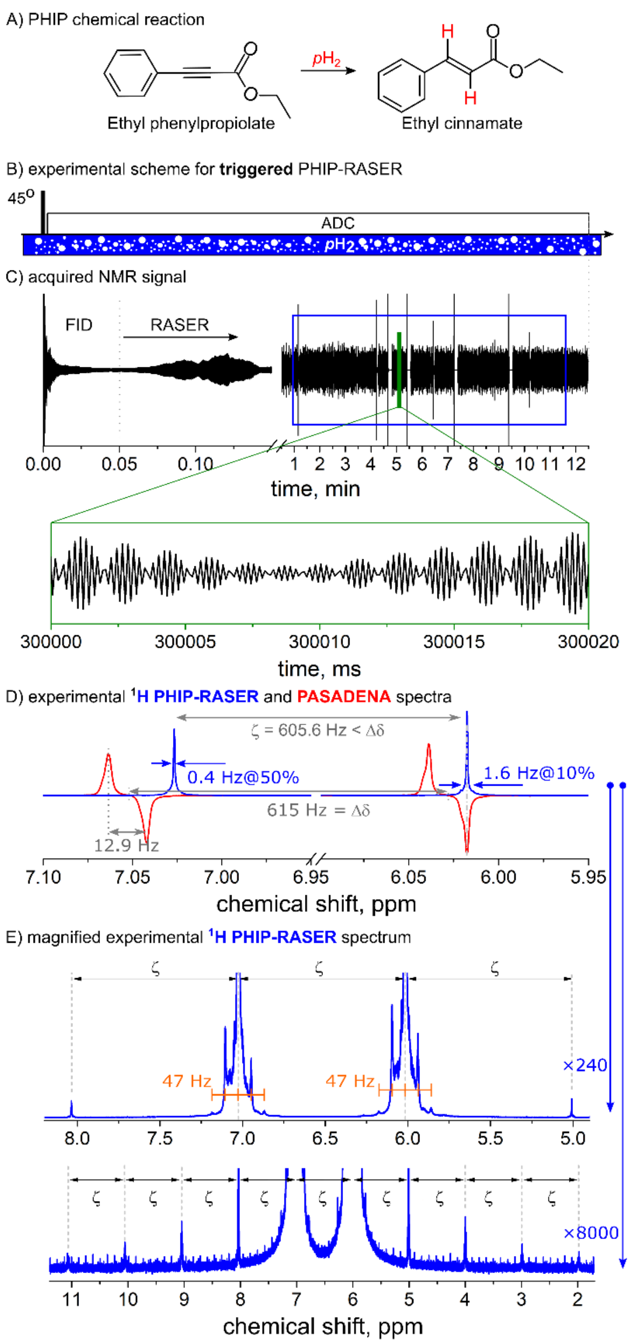

Figure 1: Triggered ^{1}H PHIP-RASER at 600 MHz. An NMR-RASER was induced by supplying pH_2 into an NMR tube with ethyl phenylpropiolate and Rh-catalyst (A) coupled to an NMR resonator in situ (B). Upon one 45° RF-excitation, NMR signal was observed for more than 12 min (C). The Fourier transform of 10.5 min data (C) exhibited two narrow lines with a full width at half maximum of 0.6 ppb (D, E; blue lines: smoothed magnitude spectrum). The right RASER line, which was acquired without frequency lock, was set to match the right negative line of a 45° PASADENA spectrum, acquired with lock and detuned probe (D, red, no radiation damping). The magnified spectrum (E) revealed several types of equidistant satellites, some of them are separated by ζ (E). Similar results were obtained for methyl proprionate (not shown). Details are given in methods.

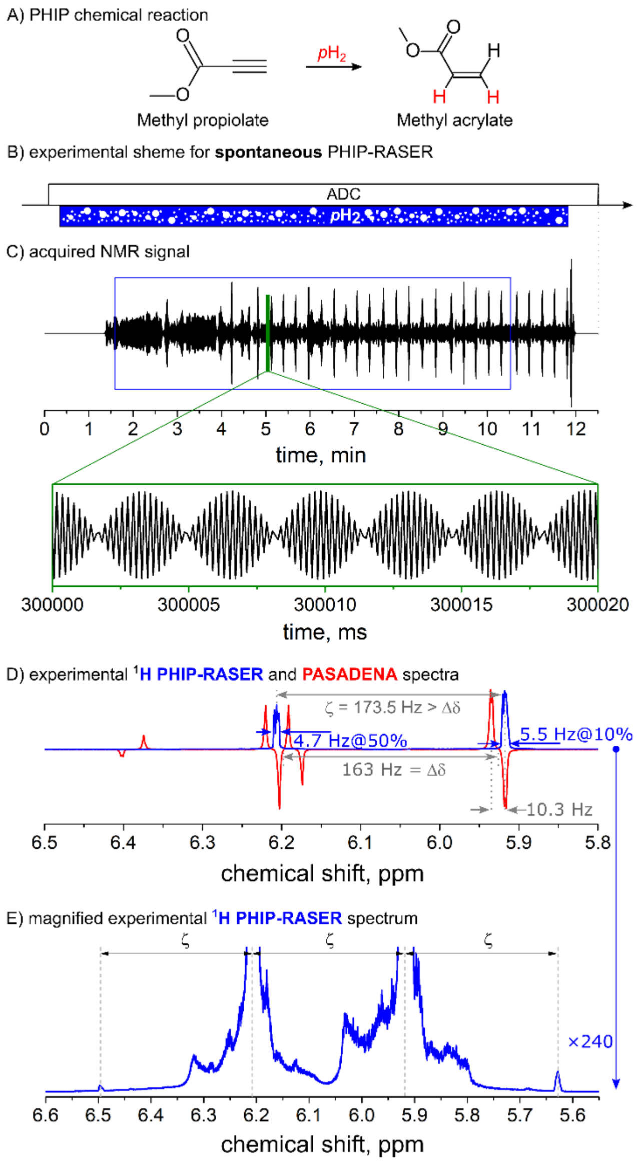

Figure 2: Spontaneous ^{1}H PHIP-RASER at 600 MHz. An NMR-RASER was induced by supplying pH_2 into an NMR tube with methyl propiolate and Rh-catalyst (A) coupled to an NMR resonator in situ (B). Without RF-excitation, spontaneous emission of NMR signal began about one minute after the onset of pH_2 supply and lasted until the pH_2 supply was stopped 11 minutes later (C). The Fourier transform of 9 min data (C) exhibited two narrow lines with a full width at half maximum of 8 ppb (D, E; blue lines: smoothed magnitude spectrum). The RASER signal was acquired without a frequency lock; instead, the right RASER line was aligned to the negative right line in a PASADENA spectrum measured with ^{2}H-lock and detuned probe (D, red). Several less prominent satellites were observed in a magnified spectrum (E). Similar results were obtained for ethyl phenylpropiolate (not shown). Details are given in methods.

10.1002/cphc.201901056

First of all, it was necessary to introduce an additional element into conventional liquid state Hamiltonian[37] to account for radiation damping:[39]

$$\widehat{\mathrm{V}}^{rd}(t,\hat{\rho}) = \boldsymbol{\omega}^{RD}\cdot\textstyle\sum_{k=1,2}\hat{\mathbf{I}}_k =$$
$$= \alpha_{RD}\textstyle\sum_{k,n=1,2}(m_{kY}(t)\,\hat{I}_{nX} - m_{kX}(t)\hat{I}_{nY}) \qquad (2)$$

This interaction can be written in analogy to the modified Bloch-Maxwell equation[40] and is similar to multi-mode RASER equations 17 and 18 from Ref. [14]. Here, $m_{kX,Y} = Tr\left(\hat{\rho}\cdot\frac{1}{2}\hat{I}^{\dagger}_{kX,Y}\right)/Tr\left(\frac{1}{2}\hat{I}_{kX,Y}\cdot\frac{1}{2}\hat{I}^{\dagger}_{kX,Y}\right)$ are the amplitudes of the transverse polarization of spin k = 1 or 2 of the density matrix $\hat{\rho}$; in general, the amplitudes are time dependent. The magnetic field induced by RD is $\boldsymbol{\omega}^{RD} = \alpha_{RD}(\sum_{k=1}^{N} m_{kY}, -\sum_{k=1}^{N} m_{kX}(t), 0)$. A radiation damping rate without polarization factor, $\alpha_{RD} = \frac{\mu_0}{4}\hbar\gamma^2\eta Q c_s$, is constant if the chemical concentrations and electronic circuitry are. On the other hand, $(\tau_{RD})^{-1}$ depends on the polarization, P, which changes continuously because of relaxation or re-hyperpolarization.

We assumed to find the simplified, two spin-½ system after hydrogenation with $p\mathrm{H}_2$ in the following state (eq 1):[22]

$$\hat{\rho}_{PASADENA} = \frac{\hat{1}}{4} - \hat{I}_{1Z}\hat{I}_{2Z} \qquad (3)$$

The supply of para-order to the system was implemented with a source operator:

$$\hat{S} = -W_{in}(t)(\hat{\mathbf{I}}_1\cdot\hat{\mathbf{I}}_2) \qquad (4)$$

No unity operator was used (see eq. 1) to keep the trace over the density matrix equal to 1. $W_{in}(t)$ is a time-dependent rate of the spin-order influx. Depending on the simulated experiment, different source operators can be used.

The addition of RD into the LvN equation makes the simulation of polarization transfer in the presence of RD[41] straightforward. Using the published SABRE models including chemical exchange, the same approach can be used to simulate SABRE-RASER.[35,42] A more detailed description of the theory and more simulation examples are given in SI. The conditions of the RASER threshold are discussed in more detail elsewhere.[14]

With these additions (eq. 2-4), we were able to reproduce all essential features observed experimentally (Fig 3 and SI): (i) two PHIP-RASER lines (Fig 3D), (ii) a distance between the RASER lines ζ that is not equal to the chemical shift difference $\Delta\delta$ and which depends on RD parameters (Fig 3D and Fig S9), (iii) an equidistant frequency-comb (Fig 3E) and (iv) a frequency shift of resonances (the latter was also reported in Refs [9,34], Fig S9).

We found that the experimental signals exhibited much stronger amplitude variations than the simulated ones. We attribute this effect to the magnetic field inhomogeneity induced by the $p\mathrm{H}_2$ supply, which was not considered in the simulations.

The same simulations were used to shed light into the classic PASADENA experiment, too. For example, an asymmetric line broadening and emission of “spontaneous”, echo-like RASER bursts were observed up to 30 s after the $p\mathrm{H}_2$ supply was stopped (see Fig S7, S11). Simulations revealed that radiation damping results in conversion of PASADENA spin order (eq 3) into longitudinal m_z – and transversal m_{xy} – magnetization (Fig S10, S11). Experimentally, this is manifested in an asymmetric broadening of spectral lines (Fig S10, SI) and RASER bursts, which may confound the interpretation of the spectra or causes inefficient polarization transfer to heteronuclei. The effect of RD on ^{1}H-PASADENA and polarization transfer to ^{13}C was recently demonstrated experimentally by Korchak et al. [41] at room temperature at fields of 1 T and 7 T.

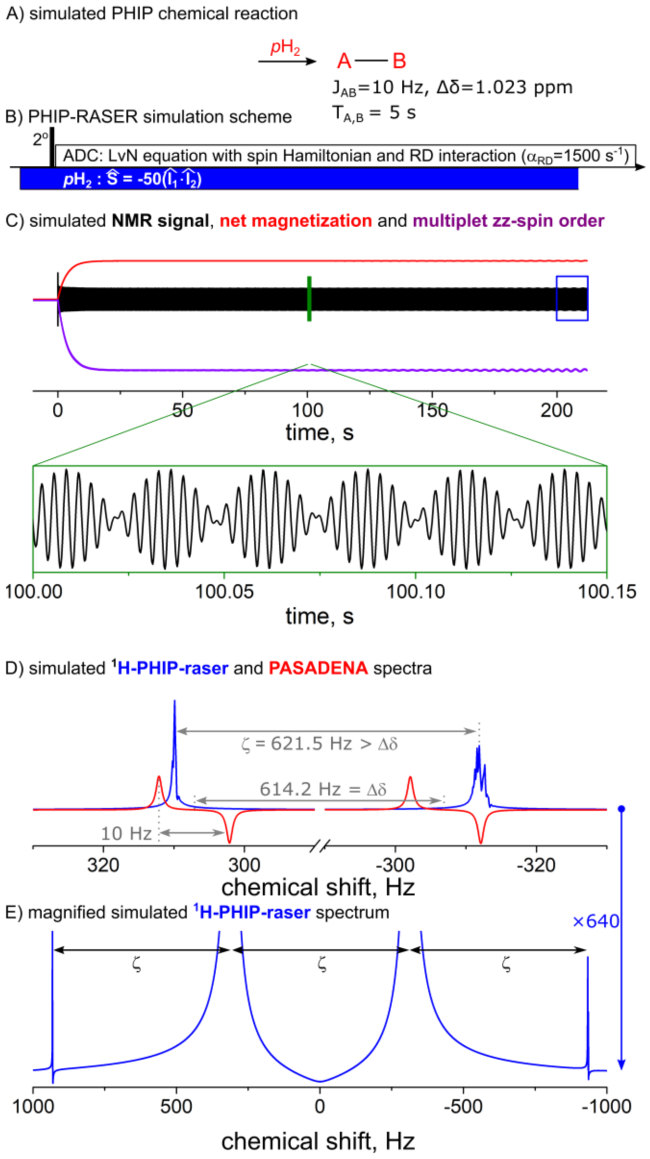

Figure 3: Simulation of ^{1}H PHIP-RASER at 600 MHz. A two spin-½ system was continuously hyperpolarized by means of PHIP (A, J = 10 Hz, $\Delta\delta$ = 1.023 ppm, relaxation times 5 s). The evolution of the system after a 2° RF-excitation was simulated using the LvN equation (C, B_0 = 14.1 T, α_{RD} = 1500 s^{-1} and W_{in} = 50 s^{-1}). Radiation damping was found to induce zz-spin order (C, violet), longitudinal (m_{1Z}, red) and transverse magnetization, the RASER signal ($m_{1X} + m_{2X}$, black line, with magnified view). The last 10 s of the transverse magnetization (C, blue square) were Fourier transformed and exhibited two lines (D, E; blue lines; magnitude, apodized with $exp(-t/2s)$). A simulated PASADENA spectrum was added for reference (D, red line, no radiation damping, FWHM = 1 Hz). Several equidistant but smaller satellites at ζ were found in the enlarged RASER spectrum (E, compare with Fig 1E,2E). The right

RASER resonance was shifted by +18 Hz to match the negative right line in PASADENA spectrum.

Conclusion

These findings establish PHIP-RASER as the first, long-lasting ^{1}H NMR-RASER at high field (and high frequencies), operating at room temperature and in the liquid state. Using standard commercial equipment, the method can be easily implemented in any NMR laboratory. The key element is a strong coupling between the resonator and hyperpolarized sample.

Moreover, with a frequency range of 10 MHz and above, PHIP-RASER is very flexible. The maximum frequency is currently limited only by the static magnetic fields available (≈ 1.2 GHz).

The long emission > 10 min allows to partially negate the detrimental effects of the strong inhomogeneity present in the sample, as narrow lines of <1 ppb were observed. Given a more homogeneous delivery of *p*H$_2$, it appears feasible to further improve on these linewidths. Simulations suggest that extremely narrow lines of a few mHz can be obtained at 600 MHz, effectively overcoming the T$_2$ limit. Note that at the same time, the full, 14-T-chemical shift dispersion is maintained. These and other applications yet to discover and implement (like RASER gyroscopes[14]) make PHIP-RASER a highly interesting effect for NMR, physics, chemistry and more.

Methods

Materials. The sample solution contained 4 mM 1,4-Bis(diphenylphosphino) butane (1,5-cyclooctadiene) rhodium(I) tetrafluoroborate (Strem Chemicals, CAS: 79255-71-3) and 60 mM ethyl phenylpropiolate (EP, Figure 1A, Sigma-Aldrich, CAS: 2216-94-6) or 100 mM methyl propiolate (MP, Figure 2A, Sigma-Aldrich, CAS: 922-67-8) dissolved in acetone-d$_6$ 99.8% (Deutero GmbH, CAS: 666-52-4). Upon hydrogenation, ethyl cinnamate (EC, Figure 1A) or methyl acrylate (MA, Figure 2A) was formed.

Experimental setup. Experiments were carried out on a 600 MHz spectrometer (Bruker Avance II) with a cryogenically cooled probe (TCI) with Q=$\nu/\Delta\nu$ ≅600.2 MHz/1.2 MHz ≅ 500 (see SI, Fig. S3) and 5 mm screw-cap NMR tubes (Wilmad). Tubes were filled with 500 µl of the sample solution. *p*H$_2$ was prepared using a home-build liquid nitrogen generator that provided a 50 % para enrichment. The gas was delivered into the spectrometer by a 1/16" polytetrafluoroethylene (PTFE) capillary. A hollow optical fibre was glued with epoxy resin to the end of the capillary and inserted into the NMR tube and solution (Molex, part. num. 106815-0026, internal diameter 250 µm and outer diameter 360 µm). A *p*H$_2$ pressure of approx. 1.2 bar (0.2 bar overpressure to atmosphere) was used to achieve a steady bubbling.

Protocol (Scheme 1). *p*H$_2$ was supplied (bubbled) into the sample solution for τ_b = 10 s to hydrogenate EP (or MP) and generate PASADENA. After that, an optional rectangular, 4 µs 45° RF-pulse was applied. All experiments were carried out at 25 °C and ambient pressure. During the experiments, some convection and diffusion occurred. *p*H$_2$ bubbling was stopped only after approx. 12 minutes of signal acquisition. Unfortunately, the NMR spectrometer did not allow for continuous data acquisition. Instead, the data was saved in 9 (Fig 1B) or 8 (Fig. 2B) blocks of 90 s and 1730768 points each. A 1-3 s delay in between the blocks caused a loss of phase coherence such that the spectra had to be calculated for each block individually. For the figures, the spectra of the first and last block in each set were omitted to exclude transient effects at the onset and end of the *p*H$_2$ injection. Magnitude RASER spectra were smoothed after averaging using a Savitzky-Golay filter with a first-order polynomial for a window of 50 points (~0.22 Hz or °0.36 ppb). No other post-processing methods such as apodization or others to improve the magnetic field stability/homogeneity (as was done in Ref. [14]) were applied.

Simulation. Simulation parameters for Fig 3: initial density matrix $\hat{\rho}(-0) = \hat{1}/4 - \hat{I}_{1Z}\hat{I}_{2Z}$, equilibrium state $\hat{\rho}_{eq} = \hat{1}/4$, J = 10 Hz, chemical shift difference 1.014 ppm, B$_0$=14.1 T, α_{RD} = 1500 s^{-1}, relaxation time 5 s and rate of polarization influx $W_{in} = 50$ s^{-1}. The simulation model is described in SI and source code is available online.[36]

Data availability. All data is available from the corresponding authors upon reasonable request.

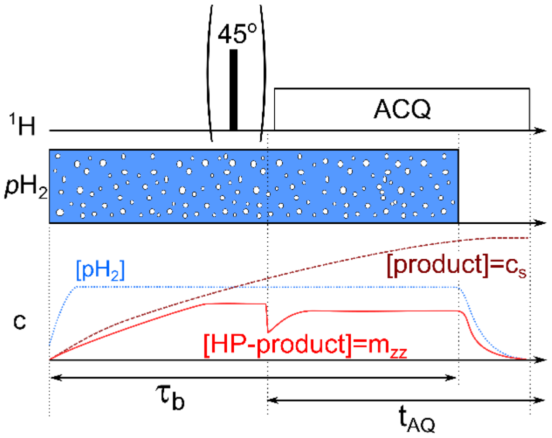

Scheme 1. Scheme of the experimental workflow (protocol 1): i) At a given time, the *p*H$_2$ supply is initiated and upheld for for a period τ_b. ii) optional excitation by hard 45° RF pulse to "trigger" RASER, and iii), signal acquisition (ACQ) in multiple blocks of 90 s each. Below, the concentrations of *p*H$_2$ (dotted blue line), total product ([product]=c$_S$, dashed wine line) and hyperpolarized product ([HP-product]=m$_{zz}$, solid red line) are plotted qualitatively. Note that *p*H$_2$ is immune to excitations with RF pulses.

Acknowledgements

We acknowledge support by the Emmy Noether Program "metabolic and molecular MR" (HO 4604/2-2), the research training circle "materials for brain" (GRK 2154/1-2019), DFG - RFBR grant (HO 4604/3-1, № 19-53-12013), the German Federal Ministry of Education and Research (BMBF) within the framework of the e:Med research and funding concept (01ZX1915C), the Cluster of Excellence "precision medicine in inflammation" (PMI 1267). Kiel University and the Medical Faculty are acknowledged for supporting the Molecular Imaging North Competence Center (MOIN CC) as a core facility for imaging in vivo. MOIN CC was founded by a grant from the European Regional Development Fund (ERDF) and the Zukunftsprogramm Wirtschaft of Schleswig-Holstein (Project no. 122-09-053).

Keywords: Coherent emission • NMR spectroscopy • parahydrogen induced polarization • Magnetic properties • RASER

[1] T. G. Walker, W. Happer, *Rev. Mod. Phys.* **1997**, *69*, 629–642.
[2] J. P. Mugler, T. A. Altes, *J. Magn. Reson. Imaging* **2013**, *37*, 313–331.
[3] M. G. Richards, B. P. Cowan, M. F. Secca, K. Machin, *J. Phys. B* **1988**, *21*, 665–681.
[4] T. E. Chupp, R. J. Hoare, R. L. Walsworth, B. Wu, *Phys. Rev. Lett.* **1994**, *72*, 2363–2366.
[5] W. Heil, C. Gemmel, S. Karpuk, Y. Sobolev, K. Tullney, F. Allmendinger, U. Schmidt, M. Burghoff, W. Kilian, S. Knappe-Grüneberg, et al., *Ann. Phys.* **2013**, *525*, 539–549.
[6] A. Abragam, J. M. Winter, *Phys. Rev. Lett.* **1958**, *1*, 374–375.
[7] S. J. Nelson, J. Kurhanewicz, D. B. Vigneron, P. E. Z. Larson, A. L. Harzstark, M. Ferrone, M. van Criekinge, J. W. Chang, R. Bok, I. Park, et al., *Sci. Transl. Med.* **2013**, *5*, 198ra108-198ra108.
[8] H.-Y. Chen, Y. Lee, S. Bowen, C. Hilty, *J. Magn. Reson.* **2011**, *208*, 204–209.
[9] D. J.-Y. Marion, G. Huber, P. Berthault, H. Desvaux, *ChemPhysChem* **2008**, *9*, 1395–1401.
[10] M. Suefke, S. Lehmkuhl, A. Liebisch, B. Blümich, S. Appelt, *Nat. Phys.* **2017**, *13*, 568–572.
[11] M. Suefke, A. Liebisch, B. Blümich, S. Appelt, *Nat. Phys.* **2015**, *11*, 767–771.
[12] J.-B. Hövener, N. Schwaderlapp, T. Lickert, S. B. Duckett, R. E. Mewis, L. A. R. Highton, S. M. Kenny, G. G. R. Green, D. Leibfritz, J. G. Korvink, et al., *Nat. Commun.* **2013**, *4*, ncomms3946.
[13] R. W. Adams, J. A. Aguilar, K. D. Atkinson, M. J. Cowley, P. I. P. Elliott, S. B. Duckett, G. G. R. Green, I. G. Khazal, J. López-Serrano, D. C. Williamson, *Science* **2009**, *323*, 1708–1711.
[14] S. Appelt, A. Kentner, S. Lehmkuhl, B. Blümich, *Progress in Nuclear Magnetic Resonance Spectroscopy* **2019**, DOI 10.1016/j.pnmrs.2019.05.003.
[15] A. N. Pravdivtsev, A. V. Yurkovskaya, H.-M. Vieth, K. L. Ivanov, R. Kaptein, *ChemPhysChem* **2013**, *14*, 3327–3331.
[16] K. L. Ivanov, A. N. Pravdivtsev, A. V. Yurkovskaya, H.-M. Vieth, R. Kaptein, *Prog. Nucl. Magn. Reson. Spectrosc.* **2014**, *81*, 1–36.
[17] A. N. Pravdivtsev, K. L. Ivanov, A. V. Yurkovskaya, P. A. Petrov, H.-H. Limbach, R. Kaptein, H.-M. Vieth, *J. Magn. Reson.* **2015**, *261*, 73–82.
[18] D. A. Barskiy, K. V. Kovtunov, I. V. Koptyug, P. He, K. A. Groome, Q. A. Best, F. Shi, B. M. Goodson, R. V. Shchepin, A. M. Coffey, et al., *J. Am. Chem. Soc.* **2014**, *136*, 3322–3325.
[19] A. Svyatova, I. V. Skovpin, N. V. Chukanov, K. V. Kovtunov, E. Y. Chekmenev, A. N. Pravdivtsev, J.-B. Hövener, I. V. Koptyug, *Chemistry – A European Journal* **2019**, *25*, 8465–8470.
[20] T. Theis, M. Truong, A. M. Coffey, E. Y. Chekmenev, W. S. Warren, *J. Magn. Reson.* **2014**, *248*, 23–26.
[21] A. N. Pravdivtsev, A. V. Yurkovskaya, H.-M. Vieth, K. L. Ivanov, *J. Phys. Chem. B* **2015**, *119*, 13619–13629.
[22] R. A. Green, R. W. Adams, S. B. Duckett, R. E. Mewis, D. C. Williamson, G. G. R. Green, *Progress in Nuclear Magnetic Resonance Spectroscopy* **2012**, *67*, 1–48.
[23] J.-B. Hövener, S. Bär, J. Leupold, K. Jenne, D. Leibfritz, J. Hennig, S. B. Duckett, D. von Elverfeldt, *NMR Biomed.* **2013**, *26*, 124–131.
[24] B. Feng, A. M. Coffey, R. D. Colon, E. Y. Chekmenev, K. W. Waddell, *Journal of Magnetic Resonance* **2012**, *214*, 258–262.
[25] S. Tam, M. E. Fajardo, *Rev. Sci. Inst.* **1999**, *70*, 1926–1932.
[26] S. Wagner, *Magn. Reson. Mater. Phy.* **2014**, *27*, 195–199.
[27] A. Gamliel, H. Allouche-Arnon, R. Nalbandian, C. M. Barzilay, J. M. Gomori, R. Katz-Brull, *Appl. Magn. Reson.* **2010**, *39*, 329–345.
[28] P. M. Richardson, A. J. Parrott, O. Semenova, A. Nordon, S. B. Duckett, M. E. Halse, *Analyst* **2018**.
[29] A. Friebel, E. von Harbou, K. Münnemann, H. Hasse, *Ind. Eng. Chem. Res.* **2019**, *58*, 18125–18133.
[30] N. Amor, P. P. Zänker, P. Blümler, F. M. Meise, L. M. Schreiber, A. Scholz, J. Schmiedeskamp, H. W. Spiess, K. Münnemann, *Journal of Magnetic Resonance* **2009**, *201*, 93–99.
[31] L. Buljubasich, M. B. Franzoni, K. Münnemann, *Top. Curr. Chem.* **2013**, *338*, 33–74.
[32] J. Eills, W. Hale, M. Sharma, M. Rossetto, M. H. Levitt, M. Utz, *J. Am. Chem. Soc.* **2019**, *141*, 9955–9963.
[33] C. R. Bowers, D. P. Weitekamp, *J. Am. Chem. Soc.* **1987**, *109*, 5541–5542.
[34] H. Desvaux, *Progress in Nuclear Magnetic Resonance Spectroscopy* **2013**, *70*, 50–71.
[35] A. N. Pravdivtsev, J.-B. Hövener, *Chem. Eur. J.* **2019**, *25*, 7659–7668.
[36] A. N. Pravdivtsev, J.-B. Hövener, *MOIN Spin Library*, (Www.Moincc.De/Method-Development/Mr/Moin-Spin-Library) UKSH, University Kiel, **2018**.
[37] A. Abragam, *The Principles of Nuclear Magnetism*, Clarendon, **1961**.
[38] P. Rovedo, S. Knecht, T. Bäumlisberger, A. L. Cremer, S. B. Duckett, R. E. Mewis, G. G. R. Green, M. Burns, P. J. Rayner, D. Leibfritz, et al., *J. Phys. Chem. B* **2016**, *120*, 5670–5677.
[39] J. Jeener, *eMagRes* **2007**, 1–37.
[40] N. Bloembergen, R. V. Pound, *Phys. Rev.* **1954**, *95*, 8–12.
[41] S. Korchak, M. Emondts, S. Mamone, B. Bluemich, S. Glöggler, *Phys. Chem. Chem. Phys.* **2019**, DOI 10.1039/C9CP05227E.
[42] S. Knecht, A. N. Pravdivtsev, J.-B. Hövener, A. V. Yurkovskaya, K. L. Ivanov, *RSC Adv.* **2016**, *6*, 24470–24477.

10.1002/cphc.201901056

RESEARCH ARTICLE

PHIP-RASER. An effect of radiation damping on hyperpolarized using para-hydrogen induced polarization (PHIP) molecules was revealed. Interaction between a highly polarized system and an NMR observation coil allowed continuous (more than 10 minutes) and coherent (less than 1 ppb line width) emission at 600 MHz using standard NMR equipment.

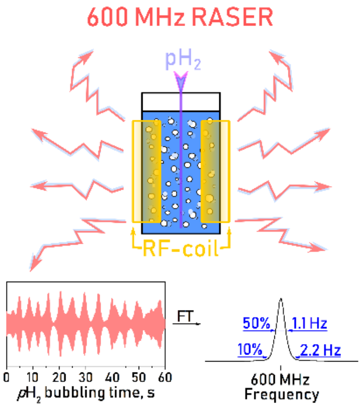

Andrey N. Pravdivtsev, Frank D. Sönnichsen and Jan-Bernd Hövener**

Page No. – Page No.

Continuous Radio Amplification by Stimulated Emission using Parahydrogen Induced Polarization (PHIP-RASER) at 14 Tesla